Incipient Fault Location Algorithm for Underground Cables

Saurabh Kulkarni, *Student Member, IEEE*, Surya Santoso, *Senior Member, IEEE*, and Thomas A. Short, *Senior Member, IEEE*

***Abstract*—Cable failure process is gradual and is characterized by a series of single-phase sub-cycle incipient faults with high arc voltage. They often go undetected and eventually result in a permanent fault. The objective of this paper is to develop a robust yet practical incipient fault location algorithm taking into account the fault arc voltage. The algorithm is implemented in the time-domain and utilizes power quality monitor data to estimate the distance to the fault in terms of the line impedance. It can be applied to locate both sub-cycle as well as permanent faults. The proposed algorithm is evaluated and proved out using field data collected from utility distribution circuits. The average absolute error in locating incipient faults for three underground cable failures analyzed in this paper was found to be 7.37%, 4.69% and 3.58%, respectively.**

***Index Terms*—Fault diagnosis, fault location, power cables, power distribution faults, time-domain analysis, underground power distribution lines.**

I. Introduction

THE INCREASED usage of underground cables has been followed by enhanced techniques for locating faults taking place on them. The prevalent cable fault location approaches depend on the voltage class and the installation of the cable system. Terminal and tracer methods [1] are applicable once a complete full-blown cable failure has occurred. However, cable failures are gradual and take place over a period of time, in contrast to other faults on overhead distribution lines [2]. Cable faults are initially incipient and self-clear, typically without the operation of an overcurrent protective device. These faults are also known as intermittent faults. Impedance-based distribution fault location methods are most commonly used with voltage and current waveforms captured by power quality (PQ) monitors [3]–[5]. These algorithms generally work in the phasor-domain and thus require duration of one or more cycles to provide reasonable location estimates [6]. Even the state-of-the-art methods like those proposed in [7], [8] work in the phasor domain. The algorithm to detect cable faults proposed in [9] utilizes one-terminal voltage and current phasor data and takes into account the cable construction and properties. However, this method is verified using only simulation data. In [10], an approach using unsupervised clustering of features through self organizing maps is taken to develop a numerical model for detecting incipient faults with voltage and current measurements as the input. Furthermore, statistical change detection algorithms are employed to determine the amount of time leading to an impending failure. Another major drawback of the present fault location methods is that they assume the circuit conditions to remain unchanged for the fault duration. The arc voltage present at the fault location is neglected. A high voltage magnitude electric arc is typically associated with incipient faults in cables [11]. A circuit modeling and injection method based time-domain approach to locate sub-cycle single line-to-ground faults is presented in [12]; however, the arc voltage at fault location is not taken into consideration. The use of arc voltage in fault location was proposed in [13], [14]. In [15], time-domain, frequency domain, as well as wavelet domain approaches to detect sustained and intermittent arcing in underground distribution systems are discussed. On the contrary, the focus of this paper is on arcing associated with sub-cycle cable faults. Given these requirements, the applicability of impedance-based algorithms is limited. The objective of this paper is to develop a robust algorithm to locate single line-to-ground incipient faults in underground cables before they become permanent.

The goals of any smart power distribution grid include improving the overall level of reliability and quality of power supplied to end users. The proposed scheme in this paper involves scanning the PQ monitor data to detect sub-cycle faults and estimating their location. Crews can be sent to repair the failing cable section, thus preventing an unplanned outage when that section breaks down permanently. This helps in achieving the goals of the smart grid enumerated above. The algorithm developed takes into account the arc voltage associated with incipient cable faults. Section II describes the characteristics of self-clearing faults in underground cables as well as the importance of arc voltage in fault detection. The proposed algorithm is implemented in the time-domain and utilizes waveform data collected by power quality monitors and relays to estimate the distance to the fault in terms of the line impedance. The algorithm uses a moving window approach, where the length of the window is governed by the fault duration. The basic algorithm remains the same for incipient and permanent faults, with some differences in the implementation. Section III details the derivation of the incipient fault location algorithm. Before applying the proposed algorithm to PQ data, the input waveforms are

Manuscript received July 03, 2012; revised December 03, 2012, April 14, 2013, August 24, 2013; accepted October 08, 2013. Date of publication April 11, 2014; date of current version April 17, 2014. Paper no. TSG-00414-2012.

S. Kulkarni and S. Santoso are with the Department of Electrical and Computer Engineering at the University of Texas at Austin, Austin, TX 78712 USA (e-mail: saurabh.k@mail.utexas.edu).

T. A. Short is with the Electric Power Research Institute (EPRI), Burnt Hills, NY 12027 USA..

Color versions of one or more of the figures in this paper are available online at http://ieeexplore.ieee.org.

Digital Object Identifier 10.1109/TSG.2014.2303483

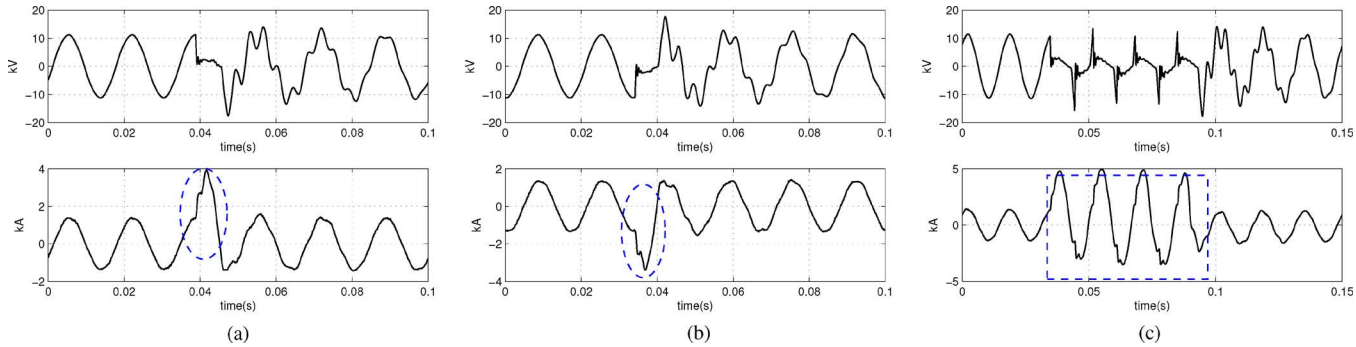

Fig. 1. Self-clearing faults leading to permanent fault in underground cable captured at the same monitor. (a) Self-clearing fault on 2008-11-12 at 19:40. (b) Self-clearing fault on 2008-11-12 at 21:11. (c) Permanent fault on 2008-11-14 at 15:51.

pre-processed to filter out the unwanted noise. Similarly, statistical techniques are applied to the output of the algorithm as a part of post-processing to obtain best possible location estimates. These pre- and post-processing techniques are discussed in Section IV. In Section V, the proposed algorithm is validated using two permanent fault cases, with known arc voltage profile and fault location, respectively. Furthermore, the accuracy of the proposed method is compared with other common impedance-based algorithms. It is found to have the best performance with an average absolute error of 12.58%. The application of the proposed algorithm to locate three actual incipient fault events and the permanent faults ensuing them is given in Section VI. The average absolute error in locating incipient faults for these cases is 7.37%, 4.69% and 3.58% respectively. Furthermore, the application of the proposed algorithm to locate faults on distribution feeders with laterals is given in Section VII, while an approach to utilize the algorithm with non-homogeneous feeders is given in Section VIII.

II. Characteristics of Self-Clearing Cable Faults

Cable failure is a gradual process characterized by precursor self-clearing or incipient faults which eventually result in a permanent fault [11]. Such a phenomenon is very common in a cable splice following moisture penetration into the splice that results in the insulation break down. An arc is produced and it evaporates the moisture, creating high pressure vapors which in turn extinguish the arc making such faults self-clearing. In this section the unique characteristics of self-clearing faults [16] are explained with the example of field data events in Fig. 1. Utility standards for detecting faults are typically in terms of the RMS current and voltage values. Since, there are no precise standards for determining sub-cycle faults, the authors have used the inspection method here.

- Fault duration is less than one cycle, generally 1/4 to 1/2 cycle. Self-clearing events shown in Fig. 1(a) and (b) represent half-cycle blips in phase B taking place on the same day nearly hour and a half apart.
- Fault generally starts near the peak of the voltage waveform. In Fig. 1(a) and (b) the fault occurs at the peak of the positive and negative voltage cycle, respectively.
- No overcurrent protective device operates because a relay generally needs more than 1/2 cycle to detect a fault.
- They are precursors to permanent faults on the same phase. The permanent fault in phase B is shown in Fig. 1(c).

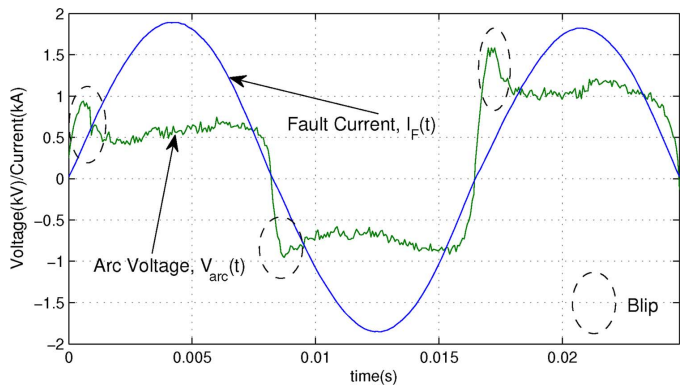

Fig. 2. Typical arc voltage and current waveforms.

- Frequency of incipient fault occurrence increases over time. There might be one or two such events initially, but their frequency can increase rapidly before they are about to turn permanent.

An arc is a self-sustained electrical discharge caused by short-circuits on the power system. It exhibits a low voltage drop and is capable of sustaining large currents. The arc voltage remains constant over a wide range of currents and arc lengths. Hence, the arc resistance is a non-linear function of the voltage. Generally, it is preferred to measure the arc in terms of the voltage rather than the resistance [17]. Typical arc voltage and current waveforms are shown in Fig. 2. The arc is sustained because of the flowing AC current. The arc cools off when this AC current reaches zero. Arc cooling decreases the ionization rate and as a result the arc resistance value increases. This results in a blip at the start of the arc voltage waveform. This blip is clearly marked in Fig. 2. Once the temperature increases with the increase in the AC current magnitude, the voltage flattens out. Presence of high odd harmonics makes the arc voltage waveform resemble a distorted square wave shape.

Extensive research has been carried out to model the characteristics of an electric arc [6]. In [18] the use of the square wave arc voltage model, in phase with the current is proposed. Further, in [13] Radojevic and Shin proposed an arc voltage model as a square wave with a superimposed harmonic content. However, the main drawback to this method is that it is in the spectral domain and does not work reliably for events less than a full cycle of fault current. Instead of modeling the arc voltage, [19] has developed an expression for arc resistance based on parameters depending on system voltage and types of insulation.

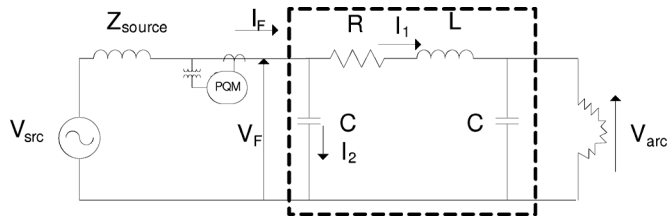

Fig. 3. Equivalent Π model of cable during a single line-to-ground fault.

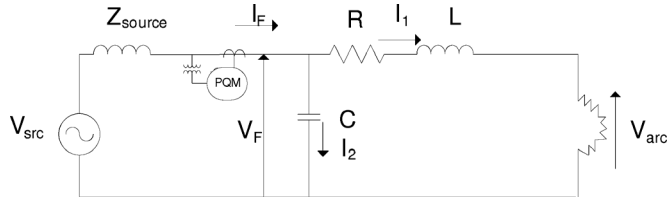

Fig. 4. Simplified model of cable during a single line-to-ground fault.

Hence, it is not possible to apply this formula when these parameters are unknown. In [18] Terzija has developed a formula for arc resistance derived under the assumption that the arc voltage is a rectangular waveform, in phase with the arc current. It requires the arc voltage gradient and arc length to be known. In this paper, we assume that only the faulted phase voltage and current waveform at the PQ monitor are available, and hence the square wave model of the arc voltage is chosen. The arc resistance is still non-linear and will change with the fault current magnitude.

The following assumptions have been made to simplify the algorithm development.

- Arc voltage has an ideal square wave shape. This implies that the arc voltage is constant irrespective of the magnitude of the fault current.
- Arc current and voltage are in phase.

In general, the arc voltage during the fault is a combination of a square wave shape and a random white noise which can be expressed as follows [14].

$$v_{\rm arc}(t) = V_{arc,mag} \cdot sign[i_F(t)] + \pounds(t) \tag{1}$$

where:

$v_{\rm arc}(t)$	is the arc voltage
$i_F(t)$	is the fault current
$\pounds(t)$	is the random zero mean white Gaussian noise
$V_{arc,mag}$	is the amplitude of the ideal square wave voltage
$sign[i_F(t)] = 1,$	for $i_F(t) > 0$ and -1 for $i_F(t) \leq 0$

Incorporating the arc voltage in the distance estimation algorithms generally improves their accuracy. This is because fault arc resistance cannot be assumed as zero (bolted fault) in all the cases especially the ones with significant arc voltage.

III. Arc Voltage Based Fault Location Algorithm

The use of arc voltage based method was proposed in [13], [20] and a simplified approach described in the previous section is used here. The algorithm is applicable to single line-to-ground faults and it estimates the arc voltage magnitude in the affected phase and the resistance and reactance to the fault. Consider that a single line-to-ground fault occurs on an underground cable. The cable, as seen from the monitoring site, can be represented by an equivalent Π model as shown in Fig. 3.

To simplify the analysis it is assumed that the capacitor on the fault side of the Π model is essentially shorted by the fault. Now the fault circuit consists only of R, L and C on the source side, as shown in Fig. 4. Note that the fault side capacitor in the Π model is a lumped representation of the distributed cable capacitance. During a low resistance or bolted fault this capacitor immediately discharges into the fault with a RC time constant typically in the microsecond or even smaller range. Most incipient faults are low resistance since they are characterized by a high fault current (otherwise they will go undetected). They have a duration typically between 1/4 to 1/2 cycle or 4 to 8 ms (for 60 Hz supply), much greater than a microsecond. After the incipient fault is self-cleared, the fault side lumped capacitor will begin to charge. Hence, the assumption of essentially shorting the fault side capacitor is justified in a sense of the time duration of the fault. However, this assumption will result in some error, though minor, in fault location.

The faulted phase voltage measured at the monitoring station, v_F, and the currents i_1 and i_2 are represented in (2).

$$\begin{aligned} v_F &= R \cdot i_1 + L \cdot \frac{di_1}{dt} + V_{arc,mag} \cdot sign(i_1) \\ i_1 &= i_F - i_2 \\ i_2 &= C \cdot \frac{dv_F}{dt} \end{aligned} \tag{2}$$

Using (2), the expression representing a single line-to-ground fault can be given as (3). As the fault current i_F is much greater than the current i_2, only the *sign* of i_F is calculated in the last term.

$$\begin{aligned} v_F = R \cdot i_F - R \cdot C \cdot \frac{dv_F}{dt} + L \cdot \frac{di_F}{dt} - L \cdot C \cdot \frac{d^2 v_F}{dt^2} \\ + V_{arc,mag} \cdot sign(i_F) \end{aligned} \tag{3}$$

Note that R and L used in (3) are the self-resistance and inductance of the line conductor, respectively. The effect of mutual coupling is not taken into consideration. Mutual coupling between the fault phase and the remaining two conductors is present, however its effect is negligible. Mutual coupling depends on the mutual inductance between the fault phase and each of the other phases, as well as the derivative of the current flowing through each unfaulted phase. Since the current in the unfaulted phases is very small compared to the fault current, mutual coupling effect will not impact the accuracy of the algorithm significantly. Furthermore, the self-impedance of a line is also known as the loop impedance and is given by $Z_{loop} = (2 \cdot Z_1 + Z_0)/3$, where Z_1 and Z_0 are the positive- and zero- sequence impedances of the line between the monitor and the fault location.

In a distribution system, the faulted phase current typically contains a component of the load current, which can lead to inaccurate fault location estimates. On the contrary, the neutral current ($i_n = i_a + i_b + i_c$) during the fault purely consists of the fault current, as the balanced load current in the three phases

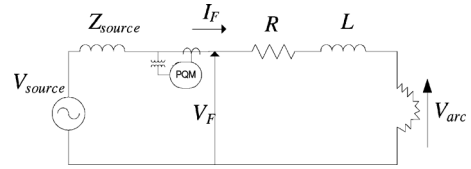

Fig. 5. Faulted phase circuit during a single line-to-ground fault.

gets canceled out. This does not get rid of the unbalanced load current. However, if the distribution circuit load model is available, the unbalanced load current can also be accounted for. As a result, the use of neutral current in the fault location algorithm yields better estimates. Hence, neutral current recorded at the monitor is used in (3) instead of faulted phase current i_F. The expression in (3) is applicable at every point of the voltage and current waveform obtained from the power quality monitors. Common sampling rates of PQ monitor waveforms are 128 or 256 samples per cycle, which results in an overdetermined system of equations. These equations can be represented in the matrix form as shown in (4). A window is defined as the number of sample points analyzed at a given time instant. A discussion on choice of window length is given in Section IV.

$$[v_F] = \left[i_n - \frac{dv_F}{dt}\frac{di_n}{dt} - \frac{d^2 v_F}{dt^2} sign(i_n) \right] \cdot \begin{bmatrix} R \\ -R \cdot C \\ L \\ -L \cdot C \\ V_{arc,mag} \end{bmatrix} \tag{4}$$

For solving (4) is written as follows.

$$\begin{aligned} &A \cdot X = b \\ &A = [a_1\ a_2\ a_3\ a_4\ a_5] \\ &a_1 = i_n, a_2 = -\frac{dv_F}{dt}, a_3 = \frac{di_n}{dt}, \\ &a_4 = -\frac{d^2 v_F}{dt^2}, a_5 = sign(i_n) \\ &[X]^T = [R \quad -R \cdot C \quad L \quad -L \cdot C \quad V_{arc,mag}] \\ &b = v_F \end{aligned} \tag{5}$$

The system of equations in (5) is overdetermined with 5 unknowns given by X. Such an overdetermined system of equations is solved using non-negative least square method [21]. This assures that only positive values of R, L, C, and $V_{\mathrm{arc,mag}}$ are considered as only positive values of these quantities hold physical significance. After computing the unknowns at one time instant the window is shifted to the next instant and the process is repeated for the entire waveform. Note that the arc voltage during the fault may vary considerably due to the tendency of the arc to elongate or shrink over a period of time. Nevertheless, the resistance and reactance to the fault should be constant during a fault. Once constant values for R and L are known, the impedance from the monitoring point to the fault location can be obtained and hence the fault location.

The faulted circuit of the cable shown in Fig. 3. can be simplified for overhead lines by neglecting the cable capacitance. The single-line diagram of this circuit is shown in Fig. 5.

The voltage at the PQ monitoring site in the time-domain, V_F for the faulted phase can be written as follows.

$$v_F = R \cdot i_F + L \cdot \frac{di_F}{dt} + V_{arc,mag} \cdot sign(i_F) \tag{6}$$

where:

v_F	is the fault phase voltage measured at PQ monitor
i_F	is the line current of the faulted phase
L	is the line inductance between monitor and fault
R	is the line resistance between monitor and fault

The solution to (6) is obtained by using the non-negative least square error method used for the solving (3). Note that the simplification presented in (6) is for demonstrating how the proposed approach can be simplified for locating faults on overhead distribution lines. For detecting underground cable faults the algorithm given by (5) is utilized throughout the paper.

Fault resistance can either arise from a foreign object in physical contact with the line conductor or from an electric arc. The proposed algorithm takes into account the non-linear fault resistance arising from the electric arc. Many fault locating algorithms assume a bolted fault [3], [4] which yields acceptable results as long as the fault resistance is low. Some algorithms lump the fault resistance term with other error terms and estimate its magnitude. In the proposed algorithm the fault resistance, apart from that resulting from the electric arc, will get lumped into the R term in (3). Hence, we utilize the L term to estimate the fault distance in terms of the reactance. This term will not be affected by the fault resistance so an accurate estimate can be obtained every time. Furthermore, after calculating the reactance to the fault, the resistance of the line conductor for that length can be determined, if the line parameters are known. The difference between this calculated line resistance and the R value from the algorithm will give the fault resistance.

IV. Pre- and Post-Processing to Improve Results

A. Pre-Processing of Input Data

The inputs to the proposed fault location algorithm are the voltage and current waveforms captured by the power quality monitor. The following pre-processing is implemented before feeding the data to the algorithm.

1) Sampling Rate Adjustment: Generally, most voltage waveforms are sampled at 256 samples per cycle in contrast to current waveforms that are sampled at 128 samples per cycle. To avoid the loss of valuable information, the current is usually up-sampled to match the voltage. Current up-sampling interpolates the in-between data points providing a waveform smoothing effect [22].

2) Smoothing and Curve Fitting: Smoothing the voltage and current waveforms before using them in the fault locating algorithm yields results with less noise. A moving average filter is applied to the voltage and current samples obtained after sampling the respective waveforms. In this method, a low-pass filter with filter coefficients equal to the reciprocal of the span is applied [22]. The number of sample points to be smoothed is given

by the span. Generally, the span is equal to 16 or 32 data samples depending on the noise in the signal.

In (4) the derivative of the neutral current i_n, as well as the first and second derivative of the faulted phase voltage v_F needs to calculated at every time instant. These derivatives are computed using the smoothing splines based technique [23]. In the first step, the current/voltage waveform during the fault is fitted as a function of time using smoothing splines. The resulting parametric piecewise cubic polynomials have a closed-loop form. In the second step, these polynomials are analytically differentiated. This technique results in the reduction of random noise when compared to simpler methods like the trapezoidal method [6], [24].

B. Post-Processing of Results

The proposed incipient fault location algorithm uses a moving window approach resulting in a range of values for fault resistance and reactance over the entire faulted portion of the waveform. Note that only the results obtained when the fault is active are valid and those when there is no fault present are to be disregarded. Most of the times, the results obtained are stable during the fault or vary within a very small range. The following post-processing methods were used to obtain the best estimates during the fault.

1) Running Mean: All the estimates obtained during the fault interval are averaged providing the best possible estimate for R and L. Reasonable results can also be obtained by simply taking the average of the highest and lowest value of the result during the fault period.

2) Back Substitution: In this method the estimated parameters are substituted back into (3). The best estimate for arc voltage, resistance and reactance to the fault will result in the least square error when the estimated voltage in the faulted phase is compared with that measured by the PQ monitor. The method can be identified as given in (7).

$$\min(e^2) = \min\left(\sum \left(v_{F,\text{estimated}} - v_{F,\text{measured}}\right)^2\right) \quad (7)$$

where $v_{F,\text{estimated}}$ is the faulted voltage estimated by substituting the parameters back into (3), $v_{F,\text{measured}}$ is the faulted voltage measured at the PQ monitor. The time instant along the waveform where the least squared error (LSE) exists is found out. The parameters at that time instant are considered to be the best estimated parameters, $R_{\text{best}} = R(t_{\text{LSE}})$, $L_{\text{best}} = L(t_{\text{LSE}})$, $V_{\text{arc,mag,best}} = V_{\text{arc,mag}}(t_{\text{LSE}})$.

3) Median Estimate: The best estimate can also be obtained by taking the median of all the estimates during the fault. The median is a robust statistic and is not influenced by outliers.

Note that either of these methods can be used for selecting the best resistance and reactance estimates to the fault.

C. Effect of Sample Window Length

Fault duration is the most important factor that determines the width of the sample window. The window length chosen has to contain the entire fault for a least one time instant. Sustained faults having duration more than a few cycles can be easily identified if the window length is less than the duration of the fault. However, using a very small window introduces noise in the results that makes the interpretation of the estimates more difficult. On the other hand, a longer window filters out most of the noise providing almost constant resistance and reactance estimates during the fault period. Thus, in case of a sustained fault, better results are obtained if a one cycle window (256 samples) is chosen. On the contrary, for incipient faults the window length is less than one cycle (generally 1/4 to 1/2 cycle) depending on the duration. The rule for window selection can be stated as: "*The window length should be less than the fault duration*."

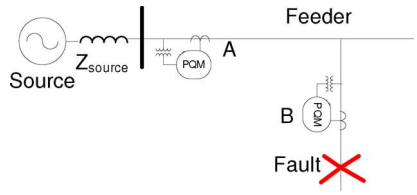

Fig. 6. Faulted distribution feeder with monitor locations.

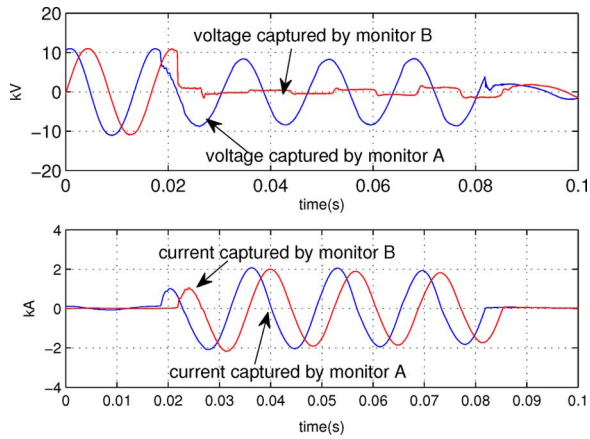

Fig. 7. Faulted phase voltage and current recorded by monitor A and B.

V. Validation of Arc Voltage Algorithm

In this section, the proposed incipient fault location algorithm is evaluated and validated using known permanent fault cases, before applying it to detect incipient cable faults. In the first step, the arc voltage estimate from the proposed algorithm is compared with a fault having known arc voltage waveform. In the second step, the algorithm is applied to detect a permanent fault with a known location. Finally, the performance of the proposed algorithm in detecting permanent faults is compared to other common impedance-based algorithms.

A. Validation Using Arcing Fault Waveforms

Fig. 6 shows a faulted 12.47 kV distribution feeder along with the monitoring stations, namely, A at the bus level and B downstream from it.

A single line-to-ground fault in phase B occurred immediately downstream from monitor B. The faulted phase voltage and current captured by monitor A and B are shown in Fig. 7. The proposed incipient fault location algorithm is applied to waveforms obtained from monitoring station A and is compared with actual faulted phase voltage waveforms obtained from monitoring station B. The arc voltage at monitor B has the classic square wave shape. This can be approximated as measured arc voltage at the fault location since monitor B is immediately upstream from the fault. Fig. 8 compares the estimates of

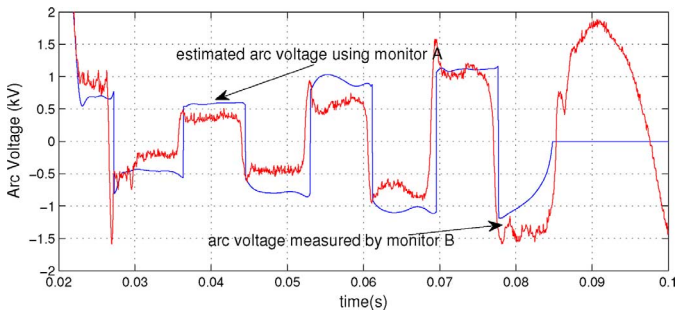

Fig. 8. Comparison between estimated and measured arc voltage.

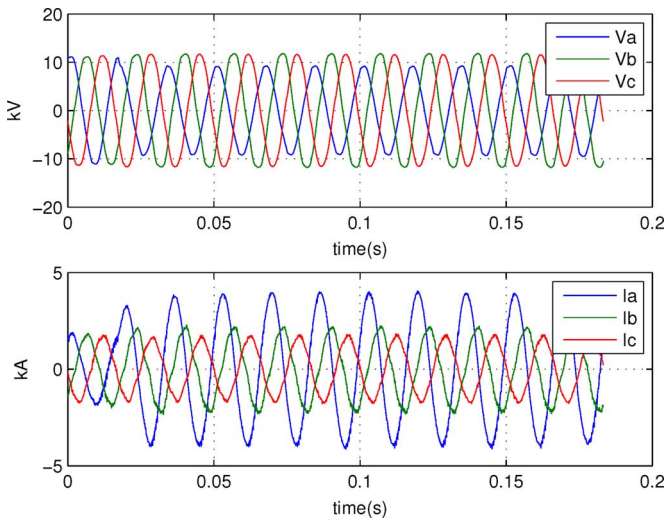

Fig. 9. Voltage and current during a permanent fault.

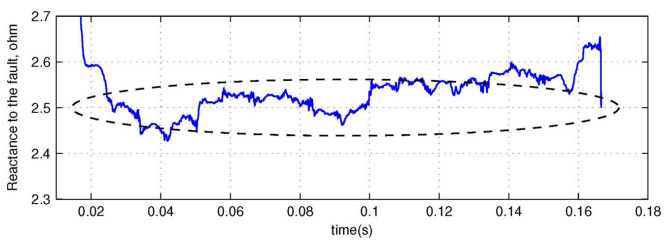

Fig. 10. Estimated reactance to the fault X_L.

arc voltage waveforms based on the substation monitor A with the actual measurement of the arc voltage from the downstream monitor B. The two are seen to match. Additionally, the arc voltage magnitude was observed to increase during the event. This can be attributed to the arc elongation phenomenon.

B. Validation Using Permanent Faults on Distribution Feeders

The application of the proposed algorithm to permanent faults is explained in this section. Permanent faults have duration of several cycles and are cleared by the operation of overcurrent protection devices. Fig. 9 shows the voltage and current waveforms captured by a power quality monitor during a permanent fault on a 13.8 kV distribution feeder. The proposed incipient fault locating algorithm is applied to this event. Resistance (R) (not shown here), reactance $X_L = 2\pi f L$ and arc voltage(V_{arc}) are computed as shown in Figs. 10 and 11, respectively. As the

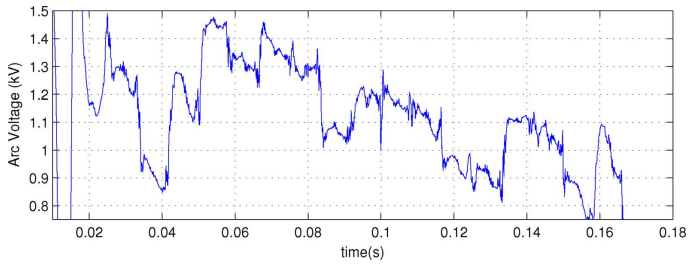

Fig. 11. Estimated arc voltage magnitude at the fault $V_{arc,mag}$.

TABLE I
REACTANCE TO FAULT ESTIMATES FOR PERMANENT FAULT

	Mean	*Median*	*Back Substitution*
X_L (Ω)	2.517	2.512	2.509
Absolute Error(Ω)	0.175	0.180	0.183
Absolute Error(%)	6.50	6.68	6.79

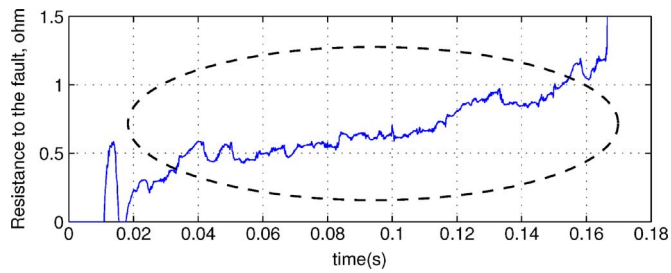

Fig. 12. Estimated resistance to the fault R.

fault has duration of several cycles the window chosen is one cycle, corresponding to 256 samples.

The three techniques for post-processing are applied to find the best estimate of the reactance to the fault. The results are summarized in Table I. The actual value of the reactance to the fault is 2.692 Ω. The error% is calculated with respect to the known fault location, since the feeder length is unknown [3]. The estimated reactance is nearly equal to the actual value and the error percentages are found to be low. In this way the accuracy of the proposed algorithm is validated using a permanent fault. Note that in the subsequent sections of the paper the running mean technique is applied to obtain the best estimates.

The resistance to the fault estimate for the event shown is Fig. 9 is also obtained when the proposed fault location approach in (5) is applied. The resistance to the fault is shown in Fig. 12. This resistance is the sum of the resistance from the PQ monitor to the fault location, any fault resistance not resulting from the electric arc and other stray resistances. As described in Section II [refer to (1)], it is more convenient to mathematically express and model the electric arc in terms of the arc voltage (Fig. 11), rather than the arc resistance.

It can be seen from Fig. 12 that the resistance value varies more than the reactance estimates shown in Fig. 10. Hence, as explained in the last paragraph of Section II, this paper uses the reactance values to estimate the fault location.

C. Comparison With Other Impedance-Based Methods

The accuracy of the proposed incipient fault locating method is compared with other impedance-based methods by analyzing

TABLE II
COMPARISON OF FAULT LOCATION METHODS

Method	*Average Absolute Error(%)*
Proposed Algorithm	12.58
Simple Ohm's Law	16.22
Absolute Value of Impedance	16.17
Loop Reactance	21.98
Takagi	17.45
Santoso et al Algorithm	14.39 to 17.48

27 actual permanent faults. The reactance to the fault is calculated using the simple ohm's law based method, absolute value of impedance method, loop reactance method, Takagi method and Santoso *et al.* algorithm [3], [4], [25]. The cumulative errors are summarized in Table II. It is seen that the proposed algorithm has the least average absolute error (12.58%) compared to rest of the methods.

D. A Note on Error in Incipient Fault Location

The algorithm developed in this paper is specifically intended for application with underground cables. The objective is to detect incipient faults and repair the cable before a full-blown permanent fault occurs. The only access the utility crew has to underground cables is through manholes. The typical distance between two manholes is a maximum of 500 ft [26]. In urban areas, which predominantly have underground power cable networks; manholes are located at every street intersection. Hence, the job of the algorithm is to predict the cable fault location such that it lies between two adjacent manholes. In other words, the fault location error percentage value is not the direct representation of the accuracy and effectiveness of the proposed method. Even if the error value is slightly higher in some cases, as long as the algorithm is able to pinpoint the location of an incipient fault between two adjacent manholes, the necessary repairs can be carried out to prevent a permanent cable fault.

VI. APPLICATION TO INCIPIENT FAULT LOCATION

The most important application of the proposed algorithm is for locating self-clearing or incipient faults. Three actual incipient cable fault cases are analyzed in detail.

A. Case 1: Two Incipient Faults Leading to Permanent Fault

A series of faulted voltage and current waveforms captured by the same monitor on a 13.8 kV distribution feeder were shown in Fig. 1. In this section, the proposed algorithm is applied to determine the location of these events in terms of the reactance to the fault from the monitor. The monitor samples the voltage at a rate of 256 samples per cycle, while the current is sampled at a rate of 128 samples per cycle. The current is up-sampled to match the voltage sampling level. Based on the discussion in Section IV, the window length chosen for the two incipient faults in Fig. 1(a) and (b) is 100 samples, i.e., between half and quarter cycle. On the other hand, for the permanent fault shown in Fig. 1(c), the window length chosen is 256 samples, or one cycle. The reactance to fault, X_L estimates for all three events are shown in Fig. 13. For this case, the actual reactance to the fault is unknown. However, assuming the estimated

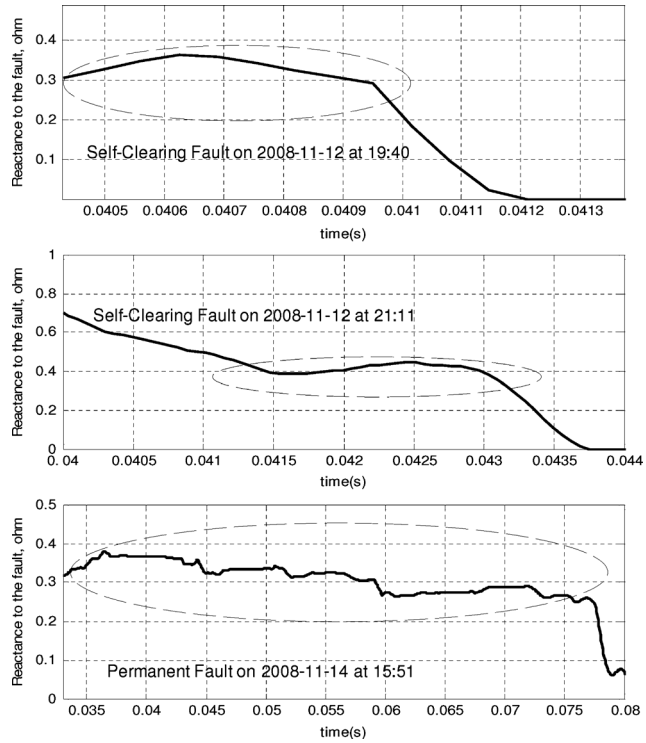

Fig. 13. Reactance to fault estimates for events shown in Fig. 1.

TABLE III
REACTANCE TO FAULT ESTIMATES FOR EVENTS IN FIG. 1

Event	*Mean Reactance Estimate(Ω)*	*Absolute Error(Ω)*	*Absolute Error(%)*
Self-Clearing Fault 1	0.344	0.0050	1.47
Self-Clearing Fault 2	0.384	0.0450	13.27
Average		0.0250	7.37
Permanent Fault	0.339	N/A	N/A

reactance during the permanent fault as the actual value, the errors for the results obtained by the precursor events are given in Table III.

The average absolute error in the reactance estimates obtained from the self-clearing faults is 7.37% or 0.0250 Ω. It can be concluded that the first two self-clearing events were precursors to the permanent fault event.

B. Case 2: Final Stages of Cable Failure

An interesting event captured by a monitor on a 13.8 kV underground cable is shown in Fig. 14. This event depicts the last stages of the cable failure process, where the incipient faults have increased in frequency and are followed by a permanent fault. The first three faults on phase C, are incipient, with a duration between half and one cycle, while the permanent fault has duration of about one and a half cycles.

The monitor samples the voltage at a rate of 256 samples per cycle, while the current is sampled at a rate of 128 samples per cycle. A 128 sample window is chosen and the reactance to fault estimates are computed as shown in Fig. 15. For this case, the actual reactance to the fault is unknown. However, assuming the estimated reactance during the permanent fault as the actual value, the errors for the results obtained by the precursor events are given in Table IV. The average absolute error in the reactance estimates obtained from the three self-

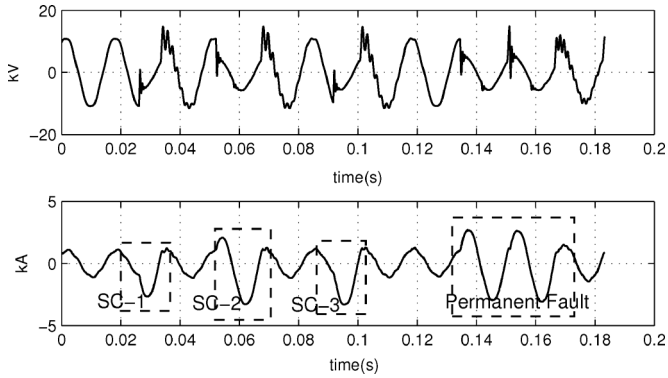

Fig. 14. Incipient cable faults on 2005-04-02 at 13:16.

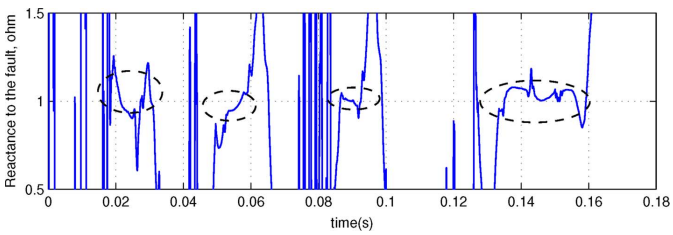

Fig. 15. Reactance to fault estimates for events shown in Fig. 14.

TABLE IV
REACTANCE TO FAULT ESTIMATES FOR EVENTS SHOWN IN FIG. 14

Event	*Mean Reactance Estimate(Ω)*	*Absolute Error(Ω)*	*Absolute Error(%)*
Self-Clearing Fault 1	0.954	0.092	8.80
Self-Clearing Fault 2	1.004	0.042	4.02
Self-Clearing Fault 3	1.033	0.013	1.24
Average		0.049	4.69
Permanent Fault	1.046	N/A	N/A

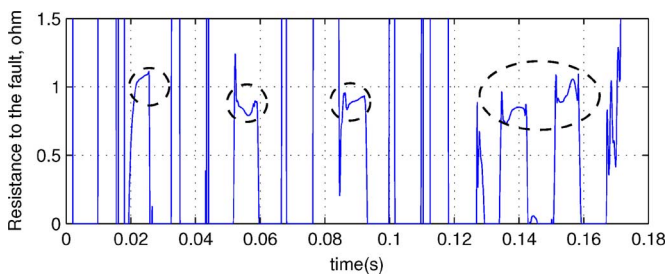

Fig. 16. Resistance to fault estimates for events shown in Fig. 14.

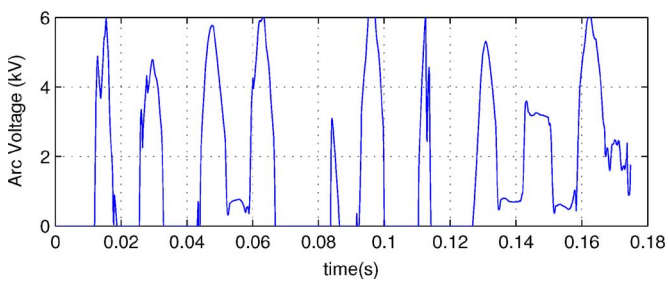

Fig. 17. Estimated arc voltage magnitude at the fault $V_{\mathrm{arc,mag}}$, for Fig. 14.

clearing faults is 4.69% or 0.049 Ω. Note that, only the estimates computed when the fault is active hold significance.

For the event in Fig. 14, the resistance to the fault estimates are shown in Fig. 16, while the arc voltage is shown Fig. 17. Note that only the arc voltage and resistance values when the fault is active are valid.

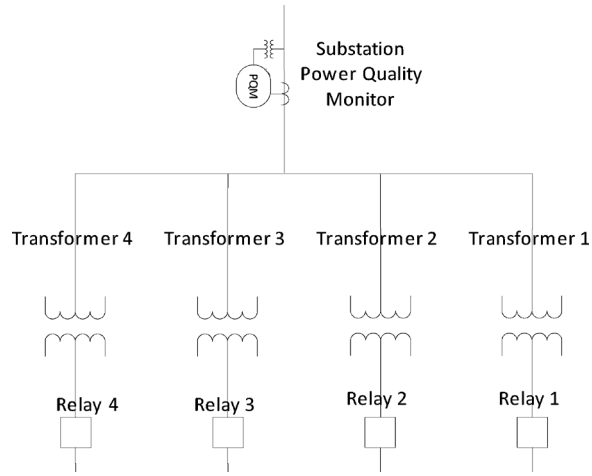

Fig. 18. Circuit diagram for Case 3.

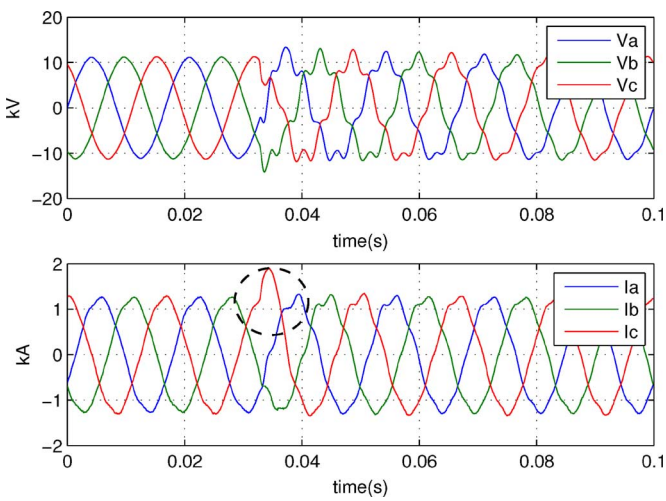

Fig. 19. First incipient fault captured by PQ Monitor on 2009-10-07.

C. Case 3: PQ Monitor and Relay Data

This section describes the location results for incipient faults recorded at a 13.8 kV distribution feeder for an underground circuit. The PQ monitor is located at the bus which has four distribution transformers connected to it as shown in Fig. 18. Since there are four transformers in service, the reactance to the fault results are divided by four from the actual estimates. Relays are located on each of the feeders. A series of self-clearing faults occurred on this underground circuit and were recorded by the PQ monitor as well as the feeder relay. The entire event had four self-clearing faults followed by a permanent fault (not shown here). The first incipient fault captured by the PQ monitor and the relay is shown in Figs. 19 and 20, respectively. The other incipient faults are similar to the first fault in the series. The cause of this event was a cable joint failure and the actual reactance to the fault is known, 0.5817 Ω from the monitor.

The sampling rate of the PQ monitor for current and voltage is 128 samples per cycle. On the other hand, the relay samples the three-phase voltage and current at a rate of 32 samples per cycle. The reactance to the fault is estimated by applying the proposed algorithm to both the PQ monitor and relay data. A half cycle window is used for the incipient faults, while a one cycle window is used for the permanent fault. The results are

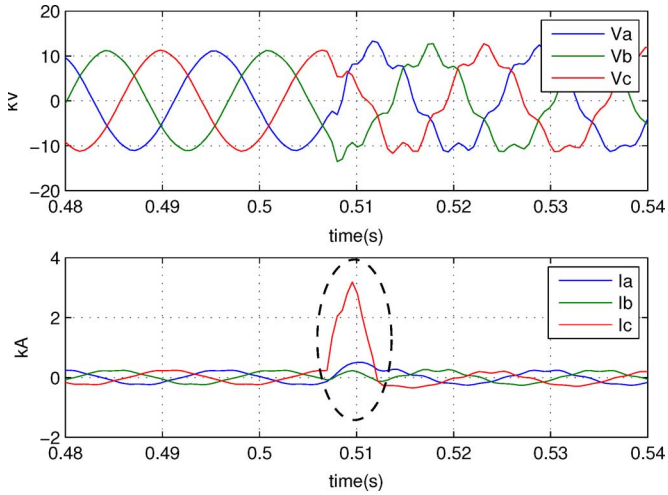

Fig. 20. First incipient fault captured by relay on 2009-10-07.

TABLE V
REACTANCE TO FAULT ESTIMATES FOR EVENTS CAPTURED BY PQ MONITOR

Event	*Mean Reactance Estimate(Ω)*	*Absolute Error(Ω)*	*Absolute Error(%)*
Self-Clearing Fault 1	0.6460	0.0064	11.05
Self-Clearing Fault 2	0.5740	0.0077	1.32
Self-Clearing Fault 3	0.5775	0.0042	0.72
Self-Clearing Fault 4	0.5888	0.0071	1.21
Average		0.0208	3.58
Permanent Fault	0.6125	0.0308	5.29

TABLE VI
REACTANCE TO FAULT ESTIMATES FOR EVENTS CAPTURED BY FEEDER RELAY

Event	*Mean Reactance Estimate(Ω)*	*Absolute Error(Ω)*
Self-Clearing Fault 1	0.8362	0.2545
Self-Clearing Fault 2	0.7112	0.1295
Self-Clearing Fault 3	0.7838	0.2021
Self-Clearing Fault 4	0.7553	0.1736
Permanent Fault	0.4446	0.1629

summarized in Tables V and VI for the reactance estimates obtained from PQ monitor and relay data, respectively. It can be seen that the reactance to the fault estimates computed using the PQ monitor data are closer to the known value with an average absolute error of 3.58% or 0.0208 Ω. The accuracy decreases for the relay estimates as the sampling rate is 32 samples per cycle as compared with the PQ monitor, which has a sampling rate of 128 samples per cycle. However, this case demonstrates that the proposed algorithm can be applied to relay data as well, to yield acceptable results. Higher the sampling rate, better the accuracy of the results.

VII. Application to Fault Location on Distribution Feeders With Laterals

A fault can occur on the main distribution feeder or on a single-phase or multi-phase lateral. The proposed fault location algorithm estimates the reactance (or distance) to fault, however, does not pinpoint the exact location on the distribution circuit. Various techniques such as relay/breaker status report, customer outage calls are commonly used by the utilities to narrow down the fault to a unique location [2], [27]. An analytical method using fault current magnitude and the distribution circuit model developed in [28] can be used in conjunction with the proposed algorithm to narrow down the fault location. The method in [28] uses the recorded fault current data, and pre-developed short-circuit current profiles to identify the feeder or lateral on which the fault might have occurred. This method is heavily influenced by the accuracy of the circuit model representing the actual distribution network as well as the fidelity of the fault current measurements. Note that the method in [28] cannot be used as a standalone technique, but can only be used to narrow down the location after an estimate is made available using the proposed algorithm.

VIII. Application to Fault Location on Non-Homogeneous Feeders

The proposed fault location algorithm is derived assuming a homogeneous cable conductor in the distribution circuit. However, this assumption is violated in practical utility distribution feeders which are constructed using different cable types. The positive- and zero-sequence impedances of the conductors vary according to the configurations. Reference [29] demonstrates that fault location methods can still be effectively applied to non-homogeneous feeders by using the line parameters of the most commonly occurring conductor type in the circuit. The errors in the fault location estimates for a distribution feeder constructed using the most commonly occurring conductor type are compared with those from the original feeder in [29]. It is found that the errors in fault location are comparable. Hence, the positive- and zero-sequence line parameters of the most commonly occurring cable conductor type in a distribution feeder can be used for fault location purposes.

IX. Conclusion

In this paper, a robust incipient fault location algorithm was developed in the time-domain, which utilizes waveform data collected by PQ monitors to estimate the fault distance in terms of the line impedance. It takes into account the arc voltage associated with incipient cable faults. This algorithm can be applied to any single line-to-ground fault as long as an appropriate window length smaller than the fault duration is chosen. Along with the proper window length, appropriate pre- and post-processing techniques have to be applied for obtaining accurate results. The efficacy of the proposed algorithm was extensively evaluated using real world data. It was demonstrated through example cases that the proposed algorithm can be used to locate multi-cycle and sub-cycle faults for monitors with sampling rates as low as 32 samples per cycle. The average error in incipient fault location was found to be below 10% in all three cable fault cases analyzed.

References

[1] E. C. I. Bascom, D. Von Dollen, and H. Ng, "Computerized underground cable fault location expertise," in *Proc. IEEE Power Eng. Soc. Transm. Distrib. Conf.*, Apr. 1994, pp. 376–382.

[2] "Distribution fault location—Prototypes, algorithms and new technologies," Electric Power Research Institute, Palo Alto, CA, USA, Tech. Rep. 1013825, Mar. 2008.

[3] *IEEE Guide for Determining Fault Location on AC Transmission and Distribution Lines*, IEEE Std. C37.114-2004, 2005.

[4] K. Zimmerman and D. Costello, "Impedance-based fault location experience," in *Proc. 2006 IEEE Rural Elect. Power Conf.*, pp. 1–16.
[5] T. Takagi, Y. Yamakoshi, M. Yamaura, R. Kondow, and T. Matsushima, "Development of a new type fault locator using the one-terminal voltage and current data," *IEEE Trans. Power App. Syst.*, vol. PAS-101, no. 8, pp. 2892–2898, 1982.
[6] M. M. Saha, J. J. Izykowski, and E. Rosolowski, *Fault Location on Power Networks*, 1st ed. New York: Springer, 2010.
[7] R. Salim, K. Salim, and A. Bretas, "Further improvements on impedance-based fault location for power distribution systems," *IET Gener., Transm., Distrib.*, vol. 5, no. 4, pp. 467–478, Apr. 2011.
[8] M.-S. Choi, S.-J. Lee, D.-S. Lee, and B.-G. Jin, "A new fault location algorithm using direct circuit analysis for distribution systems," *IEEE Trans. Power Del.*, vol. 19, no. 1, pp. 35–41, Jan. 2004.
[9] Z. Xu and T. Sidhu, "Fault location method based on single-end measurements for underground cables," *IEEE Trans. Power Del.*, vol. 26, no. 4, pp. 2845–2854, Oct. 2011.
[10] M. Mousavi and K. Butler-Purry, "Detecting incipient faults via numerical modeling and statistical change detection," *IEEE Trans. Power Del.*, vol. 25, no. 3, pp. 1275–1283, Jul. 2010.
[11] B. Clegg, *Underground Cable Fault Location*, 1st ed. New York: McGraw-Hill, 1993.
[12] C. Kim and T. Bialek, "Sub-cycle ground fault location-formulation and preliminary results," in *Proc. IEEE/PES Power Syst. Conf. Expo. (PSCE)*, Mar. 2011, pp. 1–8.
[13] Z. Radojevic and J.-R. Shin, "New one terminal digital algorithm for adaptive reclosing and fault distance calculation on transmission lines," *IEEE Trans. Power Del.*, vol. 21, no. 3, pp. 1231–1237, 2006.
[14] Z. Radojevic and V. Terzija, "Fault distance calculation and arcing faults detection on overhead lines using single end data," in *Proc. IET 9th Int. Conf. Develop. Power Syst. Protection (DPSP 2008)*, pp. 638–643.
[15] W. Charytoniuk, W.-J. Lee, M.-S. Chen, J. Cultrera, and T. Maffetone, "Arcing fault detection in underground distribution networks-feasibility study," *IEEE Trans. Ind. Appl.*, vol. 36, no. 6, pp. 1756–1761, Nov./Dec. 2000.
[16] L. Kojovic and C. W. J. Williams, "Sub-cycle detection of incipient cable splice faults to prevent cable damage," in *Proc. IEEE Power Eng. Soc. Summer Meet. 2000*.
[17] H. Ayrton, *The Electric Arc*, 1st ed. Whitefish, MT, USA: Kessinger Publ., 2007.
[18] M. Djuric and V. Terzija, "A new approach to the arcing faults detection for fast autoreclosure in transmission systems," *IEEE Trans. Power Del.*, vol. 10, no. 4, pp. 1793–1798, Oct. 1995.
[19] T. Funabashi, H. Otoguro, Y. Mizuma, L. Dube, F. Kizilcay, and A. Ametani, "Influence of fault arc characteristics on the accuracy of digital fault locators," *IEEE Trans. Power Del.*, vol. 16, no. 2, pp. 195–199, Apr. 2001.
[20] T. Short, D. Sabin, and M. McGranaghan, "Using PQ monitoring and substation relays for fault location on distribution systems," in *Proc. IEEE Rural Elect. Power Conf.*, May 2007, pp. B3–B3-7.
[21] K. Takeaki and K. Hiroshi, *Generalized Least Squares*, 1st ed. Hoboken, NJ, USA: Wiley, 2004.
[22] A. V. Oppenheim and R. W. Schafer, *Discrete-time Signal Processing*, 3rd ed. Upper Saddle River, NJ, USA: Prentice-Hall, 2010.
[23] C. De Boor, *A Practical Guide to Splines*, 1st ed. New York: Springer, 2001.
[24] S. C. Chapra and R. P. Canale, *Numerical Methods for Engineers: With Software and Programming Applications*, 4th ed. New York: McGraw-Hill, 2001.
[25] S. Santoso, R. Dugan, J. Lamoree, and A. Sundaram, "Distance estimation technique for single line-to-ground faults in a radial distribution system," in *Proc. IEEE Power Eng. Soc. Winter Meet. 2000*.
[26] A. J. Pansini, *Guide to Electrical Power Distribution Systems*, 6th ed. Boca Raton, FL, USA: CRC, 2005.
[27] "Distribution fault location—Field data and analysis," Electric Power Research Institute, Palo Alto, CA, USA, Tech. Rep. 1012438, Dec. 2006.
[28] S. Das, S. Kulkarni, N. Karnik, and S. Santoso, "Distribution fault location using short-circuit fault current profile approach," in *Proc. IEEE Power Energy Soc. Gen. Meet.*, Jul. 2011, pp. 1–7.
[29] S. Kulkarni, N. Karnik, S. Das, and S. Santoso, "Fault location using impedance-based algorithms on non-homogeneous feeders," in *Proc. IEEE Power Energy Soc. Gen. Meet.*, Jul. 2011, pp. 1–6.

Saurabh Kulkarni received his M.S. and Ph.D. degrees from the Department of Electrical and Computer Engineering, University of Texas at Austin, TX, USA, in 2009 and 2012, respectively. His research interests are in power quality and distribution fault analysis.

Surya Santoso (M'96–SM'02) received the M.S.E. and Ph.D. degrees in electrical and computer engineering from the University of Texas at Austin, TX, USA, in 1994 and 1996, respectively. From 1997 to 2003, he was a Consulting Engineer with Electrotek Concepts. Currently, he is an Associate Professor in the Department of Electrical and Computer Engineering at the same university. His research interests include power quality, power systems, and wind power.

Thomas A. Short (M'90–SM'98) received the M.S.E.E. degree from Montana State University, Bozeman, MT, USA, in 1990. He is a Senior Engineer with EPRI, Burnt Hills, NY, USA. Before that, he was with Power Technologies, Inc., for ten years. He authored the *Electric Power Distribution Handbook* (CRC, 2004). Mr. Short led the development of IEEE Std. 1410–1997, as Chair of the IEEE Working Group on the Lightning Performance of Distribution Lines. For this effort, he was awarded the 2002 Technical Committee Distinguished Service Award.